Vol. 15 № 4 Trans. Nonferrous Met. Soc. China Aug. 2005

Article ID: 1003-6326(2005)04-0823-05

Synthesis and high-temperature performance of Ti substituted α-Ni(OH)$_2$ ①

LIU Hong-bing(刘宏兵), XIANG Lan(向 兰), JIN Yong(金 涌)
(Department of Chemical Engineering, Tsinghua University, Beijing 100084, China)

Abstract: Ti substituted α-Ni(OH)$_2$($c = 2.121$ nm, $a = 0.307$ nm) with perfect high-temperature performance was prepared by the co-precipitation method. The effects of Ti addition on the structure and the electrochemical properties were investigated. The results indicate that the substitution of Ti for Ni leads to the conversion of β-Ni(OH)$_2$ to α-Ni(OH)$_2$ and the increase of the inter layer distance along c-axis from 0.464 nm to 0.707 nm. Infrared study reveals that more anions(SO_4^{2-} and CO_3^{2-} ions) and H_2O exist in the Ti substituted α-Ni(OH)$_2$. The discharge capacity of the Ti substituted α-Ni(OH)$_2$ is 210 mA·h/g at 20 ℃ and reaches up to 270 mA·h/g at 80 ℃ owing to the inhibition of the oxygen evolution at high temperature.

Key words: α-Ni(OH)$_2$; titanium; structure; high temperature performance

CLC number: TM 912.2 **Document code:** A

1 INTRODUCTION

The development of electric and hybrid vehicles is proceeding against the backdrop of environmental problems, and nickel-metal hydride batteries(MH/Ni) with high output, high energy density, low cost and long durability are being considered the alternative cardinal components for these vehicles. In recent years, synthesis of Ni(OH)$_2$ powder with perfect high-temperature electrochemical properties has gotten more and more attention since the low charge acceptance of nickel electrode at high temperature becomes one of the main problems hindering the application of MH/Ni batteries in the electric vehicles.

There are two possible reactions in the charging process of the commercial β-Ni(OH)$_2$ positive electrode:

Oxidation,

$$\beta\text{-Ni(OH)}_2 + OH^- \leftrightarrow \beta\text{-NiOOH} + H_2O + e \qquad (1)$$

Oxygen evolution,

$$4OH^- \rightarrow O_2 + 2H_2O + 4e \qquad (2)$$

The oxidation potential is lower than the oxygen evolution potential at room temperature. But the oxygen evolution potential decreases rapidly at higher temperature[1], leading to the occurrence of the by-reaction of the oxygen evolution and the decrease of the charge efficiency. Many work has been done to improve the charge efficiency at high temperature, e.g., the design of the advanced cooling system to keep the electrode at a relatively low temperature, the addition of Co or Y to reduce the oxidation potential of β-Ni(OH)$_2$[2, 3], the addition of ZnO, CdO, CaO, Y_2O_3, Yb_2O_3 and Lu_2O_3 to raise the oxygen evolution potential[4-6], and the addition of NaOH or LiOH to KOH electrolyte to raise the oxygen evolution potential[7], etc. Even though much work has been done on the commercial β-Ni(OH)$_2$/β-NiOOH cycle, there is still no effective way to produce Ni(OH)$_2$ with desirable charge efficiency at temperature above 50 ℃. Another deficiency in β-Ni(OH)$_2$ is the limitation of capacity and the volume swelling[8], which might be solved if the stable cycle between α-Ni(OH)$_2$ and γ-NiOOH could be realized[9-14].

Because α-Ni(OH)$_2$ is labile in alkaline media, experiments by partial substitution of trivalent cations such as Al^{3+}, Co^{3+}, Fe^{3+} and Mn^{3+} have been made[9-14]. But up to now little work has been concerned with the high-temperature behavior of α-Ni(OH)$_2$.

In the present work, the Ti substituted α-Ni(OH)$_2$ with a perfect electrochemical behavior at high temperature was synthesized via co-precipitation route using soluble Ti^{3+} as the doped element. The structure was characterized by XRD and FT-IR, the charge and discharge performance at high temperature was evaluated and discussed.

2 EXPERIMENTAL

2.1 Preparation

α-Ni(OH)$_2$ was prepared by adding(0.5 mL/

---

① **Received date:** 2004-12-02; **Accepted date:** 2005-03-21

Correspondence: XIANG Lan, Associate Professor; Tel/Fax: +86-10-62772051; E-mail: xianglan@flotu.org

min) 100 mL of a mixing solution containing 0.8 mol/L $NiSO_4$ and 0.1 mol/L $TiCl_3$ to 200 mL of 1.0 mol/L LiOH solution, while stirring at 20 ±2 ℃. The suspension was then aged for 12 h, filtered, washed with distilled water to pH of 7 − 8 and dried at 110 ±2 ℃ for 12 h.

β-$Ni(OH)_2$ was synthesized by simultaneous addition(0.5 mL/min) of 100 mL of the mixing solution (containing 2.0 mol/L NaOH and 2.0 mol/L NH_4OH) and 100 mL of the 1.0 mol/L $NiSO_4$ solution to 200 mL of the buffer solution containing 0.4 mol/L NH_4OH and 0.015 mol/L $(NH_4)_2SO_4$ (pH= 10.5), while stirring at 20 ±2 ℃. The pH of the reaction solution was monitored in situ by a pH meter and controlled in the range of 10.5 −11.5 by adjusting the dropping rate of the alkaline solution containing NaOH and NH_4OH. The suspension was then aged for 12 h, filtered, washed with distilled water to pH 7 − 8 and dried at 110 ±2 ℃ for 12 h.

2.2 Preparation of $Ni(OH)_2$ electrode

The paste containing 90% $Ni(OH)_2$ and 10% $Co(OH)_2$ was inserted into the nickel foam with porosity over 95%, using 0.5% carboxymethyl and 1% polytetrafluorothylene as the binder agents. After drying at 110 ℃ for 2 h, the above electrode was sandwiched between two identical Ni foam electrodes and pressed under 60.0 MPa for 5 min.

2.3 Evaluation of electrochemical properties

The $Ni(OH)_2$ electrode was immersed into 7.0 mol/L NaOH + 0.3 mol/L LiOH electrolyte, using the Ni foam (with the same size as the positive electrode) as the negative electrode and the Hg/HgO (7.0 mol/L NaOH + 0.3 mol/L LiOH) as the reference electrode. The positive electrode was charged and discharged at a constant current in the temperature range of 20 − 80 ℃. The cell was then charged at 30 mA/g for 15 h, rested for 1 h, and discharged at 90 mA/g until the potential decreased to 0.1 V. The charge-discharge experiment was re-cycled for two times and the discharge capacity in the second cycle was detected.

2.4 Characterization

The structures and the functional groups of the samples were characterized by X-ray diffraction (XRD, model D/max, Rigaku, Japan) and Fourier Transform Infrared spectrometry (FT-IR, model Nicolet 560, Nico, American), respectively. The contents of Ni and Ti were determined by ethylenediaminetetraacetic acid (EDTA) titration.

3 RESULTS AND DISCUSSION

Fig. 1 shows the influence of Ti substitution on the XRD patterns of $Ni(OH)_2$. In the absence of Ti, β-$Ni(OH)_2$ with an inter-layer distance of c = 0.464 nm along c-axis (according to the (001) peak at 19.1°, $c = d_{(001)}$) and a Ni-Ni atom distance of a = 0.313 nm (according to the (110) peak at 59.1°, $a = 2d_{(110)}$) was formed. In the presence of Ti, α-$Ni(OH)_2$ (c = 2.121 nm according to the (003) peak at 12.5° and a = 0.307 nm according to the (110) peak at 60.3°, $c = 3d_{(003)}$, $a = 2d_{(110)}$) formed since the occurrence of the large asymmetric peak at 34.0° is the feature of the turbo-stratic structure in α-$Ni(OH)_2$[15]. The change of the lattice parameters may be connected with the insertion of Ti into the $Ni(OH)_2$ lattice. The sharper XRD peaks in sample (a) indicates that the crystallization of β-$Ni(OH)_2$ is more perfect than that of the Ti substituted α-$Ni(OH)_2$.

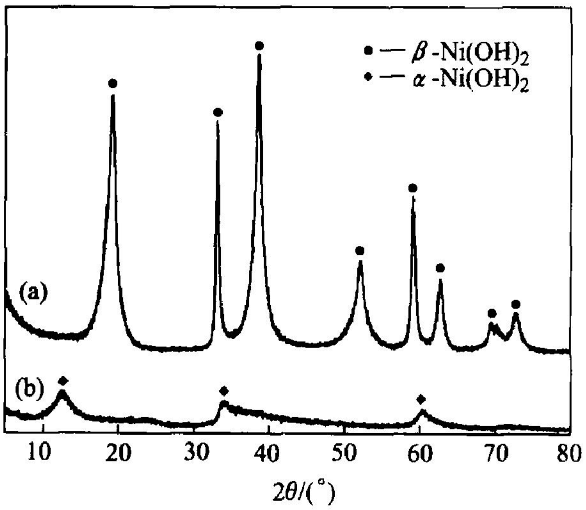

Fig. 1 XRD patterns of $Ni(OH)_2$ without Ti(a) and with Ti(b)

The FT-IR spectra of the β-$Ni(OH)_2$ and the Ti substituted α-$Ni(OH)_2$ are shown in Fig. 2. The broad band in the region of 3 000 − 3 800 cm^{-1} is ascribed to the stretch vibration of O—H. In the case of Ti substituted α-$Ni(OH)_2$, the peak at 1 645 cm^{-1} is the bend vibration of H_2O, the peaks at 1 490 cm^{-1} and 1 382 cm^{-1} are the υ_3 vibration of CO_3^{2-} in D_{3h} symmetry, the peaks at 1 120 cm^{-1} (υ_3 vibration) and 1 038 cm^{-1} (υ_3 vibration) are attributed to the interaction between SO_4^{2-} in C_{3v} symmetry and the metallic cations (Ni^{2+} and Ti^{3+}). The average inter-layer distance is 0.707 nm according to the location of the (003) peak (2θ = 12.5°), implying that most of the SO_4^{2-} might be adsorbed on the surface of $Ni_{1-x}Ti_xO_2$ layers since the inter-layer distance should be in the range of 0.88 − 0.94 nm if SO_4^{2-} is intercalated into the inter-layers[16]. Moreover, the distribution of the inter-layer distance along c-axis is in the range of 0.564 − 0.954 nm according to the (003) peak in Fig. 1 (occurring in the 2θ range of 9.3°− 15.7°), indicating the partial intercalation of SO_4^{2-} ions into the inter-layers to compensate the positive charge caused by the partial substitution of Ni^{2+} by Ti^{3+}. In the case of β-Ni(OH)$_2$, the sharp peak at 3 650 cm^{-1} corresponds to the free OH group in β-Ni(OH)$_2$ phase[17]. The bigger peak areas for O—H and CO_3^{2-} in the Ti substituted α-Ni(OH)$_2$ than in β-Ni(OH)$_2$ indicate that more anions (SO_4^{2-} and CO_3^{2-} ions) exist in the Ti substituted α-Ni(OH)$_2$ to compensate the positive charge induced by Ti^{3+}, more water exist between the inter-layers of the Ti substituted α-Ni(OH)$_2$ because of the larger inter-layer distance.

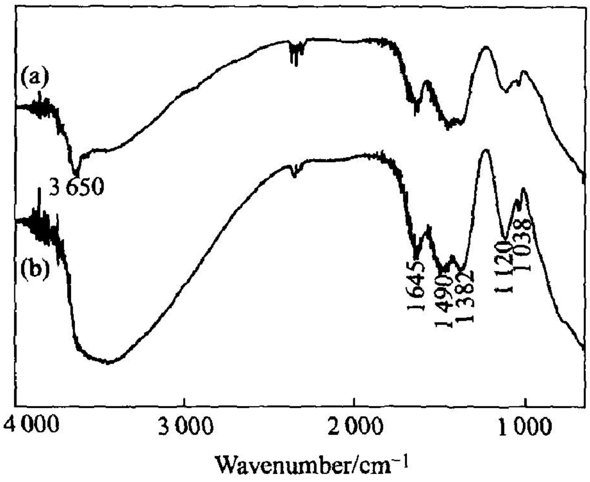

Fig. 2 IR spectra of α-Ni(OH)$_2$(a) and Ti substituted α-Ni(OH)$_2$(b)

The charge-discharge curves of β-Ni(OH)$_2$ and Ti substituted α-Ni(OH)$_2$ at different temperatures are shown in Fig. 3, and the corresponding oxidation potential, the oxygen evaluation potential and the discharge capacity originated from Fig. 3 are shown in Fig. 4 and Fig. 5, respectively.

The data in Fig. 3 indicate that the partial substitution of Ni^{2+} by Ti^{3+} (Ni47. 7%, Ti6. 6%, mass fraction) changes the charge and discharge behaviors. The lower oxidation potential (the average charge potential[6]) in Ti substituted α-Ni(OH)$_2$ indicates the improvement of the charge behavior in α-Ni(OH)$_2$, which may be attributed to the change of structure since the increase of the inter layer distance and the water content are favorable to the acceleration of the diffusion of the protons[9]. The lower charge potentials at higher temperature in both of β-Ni(OH)$_2$ and α-Ni(OH)$_2$ samples indicates that the increase of temperature also accelerates the diffusion of protons. The charge curves for both α-Ni(OH)$_2$ and β-Ni(OH)$_2$ exhibit two plateaus at 20 ℃. The primary one is assigned to the oxidation of Ni^{2+} as shown in reaction (1); the second plateau represents the evolution of oxygen, corresponding to the visual formation of bubbles on the nickel electrode. In the case of β-Ni(OH)$_2$, the rise of temperature leads to the gradual disappearance of the second plateau and the earlier evaluation of bubbles, indicating that the oxidation of Ni^{2+} and the evolution of oxygen proceeds simultaneously[6].

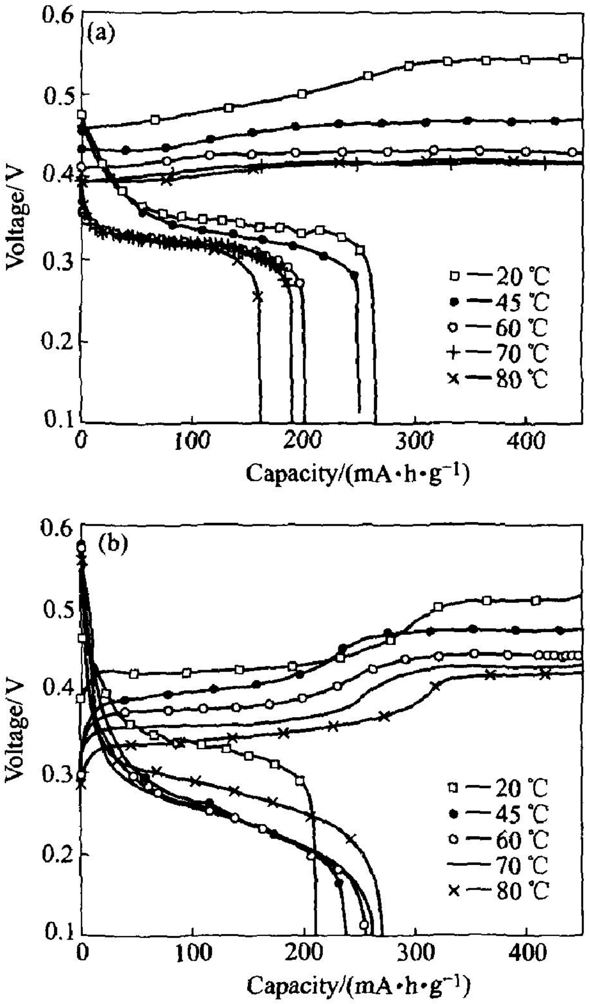

Fig. 3 Charge—discharge curves of β-Ni(OH)$_2$(a) and Ti substituted α-Ni(OH)$_2$(b)

The influence of temperature on the oxidation potential (or the average charge potential) and the oxygen evolution potential (defined as the maximal charge potential) are shown in Fig. 4. With the increase of the temperatures from 20 ℃ to 80 ℃, the difference between the oxidation potential and oxygen evolution potential disappears gradually in the case of β-Ni(OH)$_2$ but keeps relatively stable in the case of α-Ni(OH)$_2$. The oxygen evolution potential for α-Ni(OH)$_2$ is 5－10 mV higher than that of β-Ni(OH)$_2$ in the temperature range of 45 ℃ to 80 ℃.

The evolution of oxygen from the nickel electrode in the alkaline medium is as follows[18, 19]:

$$OH^- \leftrightarrow OH_{(ads)} + e \qquad (3)$$

$$OH_{(ads)} + OH^- \leftrightarrow O^-_{(ads)} + H_2O \qquad (4)$$

$$O^-_{(ads)} + 2NiOOH \leftrightarrow 2NiO_2 + H_2O + e \qquad (5)$$

$$2NiO_2 + OH_{(ads)} \leftrightarrow NiOOH + O_{(ads)} \qquad (6)$$

$$2O_{(ads)} \leftrightarrow O_2 \qquad (7)$$

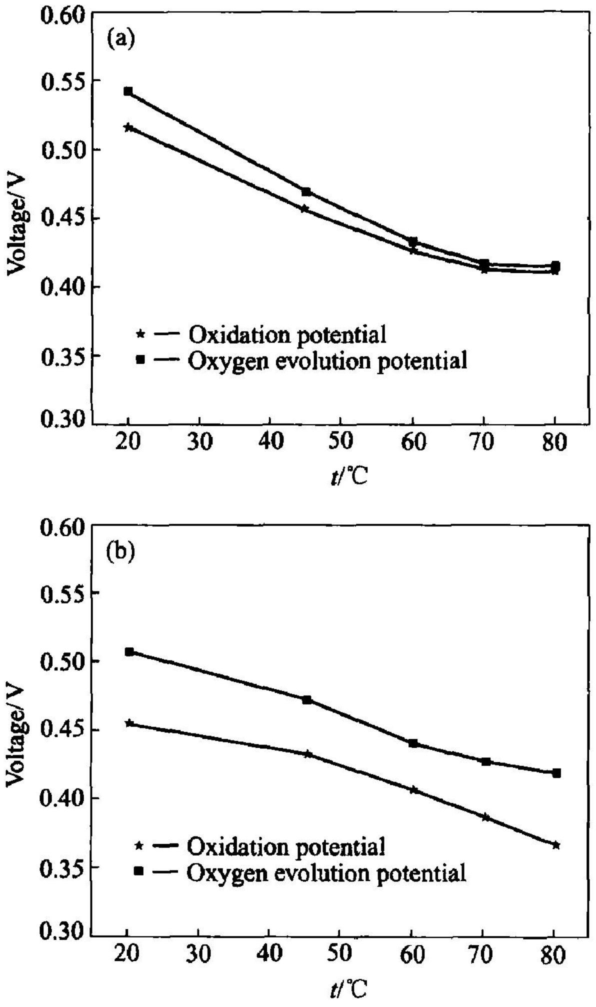

Fig. 4 Variation of oxidation potential and oxygen evolution potential with temperature
(a) —β-Ni(OH)$_2$;
(b) —Ti substituted α-Ni(OH)$_2$

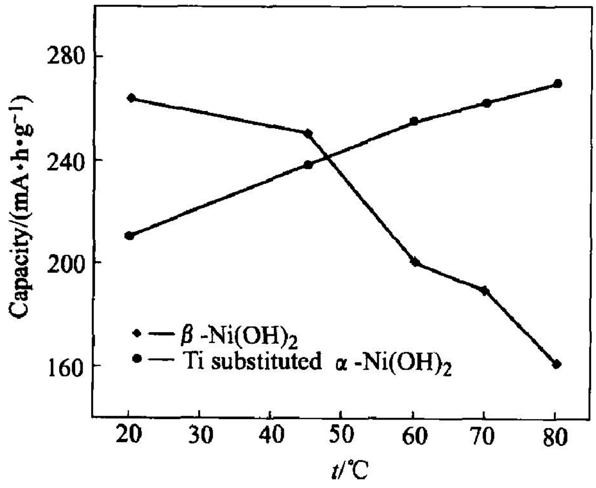

Fig. 5 Variation of discharge capacity with temperature

The evolution of oxygen occurs on the surface of the oxide layer (NiOOH). It was reported that the metal oxides with s^2p^6 metallic electron configuration (such as CaO and Y_2O_3) can act with NiOOH, leading to the inhibition of the electron transfer and the increase of the oxygen evolution potential[4, 5]. The higher oxygen evolution potential of the α-Ni(OH)$_2$ may be connected with the existence of Ti since Ti^{3+} can be easily oxidized to Ti^{4+} (with s^2p^6 electron configuration) in the charge process.

The influence of temperature on the discharge capacities is shown in Fig. 5. With the increase of temperature from 20 ℃ to 80 ℃, the discharge capacity decreases from 264 mA • h/g to 161 mA • h/g in β-Ni(OH)$_2$. The dramatic decline of the discharge capacity in the temperature range of 45 - 60 ℃ may connect with the decrease of the difference between the oxidation potential and the oxygen evolution potential. In the case of the Ti substituted α-Ni(OH)$_2$, the discharge capacity is about 210 mA • h/g at 20 ℃ and reached up to 270 mA • h/g (about 1.22 electron transfer per nickel atom) at 80 ℃, indicating that the increase of temperature is favorable to the oxidation of Ni^{2+} to Ni^{4+}.

4 CONCLUSIONS

Ti substituted α-Ni(OH)$_2$ with a perfect electro-chemical properties at high temperature was synthesized at room temperature via co-precipitation route, using $NiSO_4$ and $TiCl_3$ as the reactants and LiOH as the precipitation agent. The substitution of Ti for Ni leads to the conversion of β-Ni(OH)$_2$ to α-Ni(OH)$_2$ and the increase of the inter layer distance along *c*-axis from 0.464 nm to 0.707 nm. The discharge capacity of the Ti substituted α-Ni(OH)$_2$ can reach up to 270 mA • h/g (about 1.22 electron transfer per nickel atom) at 80 ℃ owing to the inhibition of the oxygen evolution at high temperature.

REFERENCES

[1] Kibria M F, Mridha M S. Electrochemical studies of the nickel electrode for the oxygen evolution reaction [J]. International Journal of Hydrogen Energy, 1996, 21(3): 179 - 182.

[2] Unates M E, Folquer M E. The influence of foreign cations on the electrochemical behavior of the nickel hydroxide electrode [J]. Journal of the Electrochemical Society, 1992, 139(10): 2697 - 2704.

[3] MI Xin, JIANG Chang-yin, GENG Ming-ming, et al. Synthesis and high-temperature charge/discharge performance of the Y^{+3}-doped spherical Ni(OH)$_2$ [J]. Chinese Journal of Battery, 2004, 34(1): 13 - 15.

[4] Oshitani M, Takayyanma T, Takashima K, et al. A study on the swelling of a sintered nickel hydroxide electrode [J]. Journal of Applied Electrochemistry, 1986, 16(3): 403 - 408.

[5] Akihiro M, Hirokazu K, Yoshio M, et al. Alkaline Storage Battery [P]. EP0923146A1, 1999.

[6] Oshitani M, Watada M, Shodai K, et al. Effect of lanthanide oxide additives on the high-temperature charge acceptance characteristics of pasted nickel elec-

trodes [J]. Journal of the Electrochemical Society, 2001, 148(1): A67-A73.

[7] Ezhov B B, Malandin O G. Structure modification and change of electrochemical activity of nickel hydroxide [J]. Journal of the Electrochemical Society, 1991, 138 (4): 885-889.

[8] Bode H, Dehmelt K, Witte J. Zur kenntnis der nickel hydroxidelektrode—Ⅰ. Uber das nickel(Ⅱ)-hydroxidhydrat [J]. Electrochimica Acta, 1966, 11: 1079-1087.

[9] Sugimoto A, Ishida S, Hanawa K. Preparation and characterization of Ni/Al-layered double hydroxide [J]. Journal of the Electrochemical Society, 1999, 146 (4): 1251-1255.

[10] ZHANG Heng-bin, LIU Han-san, CAO Xue-jing, et al. Preparation and properties of the aluminum-substituted α-Ni(OH)$_2$ [J]. Materials Chemistry and Physics, 2003, 79: 37-42.

[11] HU Wei-kang, Noréus D. Alpha nickel hydroxides as lightweight nickel electrode materials for alkaline rechargeable cells [J]. Chemistry of Materials, 2003, 15(4): 974-978.

[12] Faure C, Delmas C, Willmann P. Electrochemical behavior of α-cobalted nickel hydroxide electrodes [J]. Journal of Power Sources, 1991, 36: 497-506.

[13] Guerlou L D, Delmas C. Structure and properties of precipitated nickel-iron hydroxides [J]. Journal of Power Sources, 1993, 45: 281-289.

[14] Demourgues L G, Delmas C. Electrochemical behavior of the manganese-substituted nickel hydroxides [J]. Journal of the Electrochemical Society, 1996, 143(2): 561-566.

[15] Faure C, Delmas C. Preparation and characterization of cobalt-substituted α-nickel hydroxide stable in KOH medium(Part Ⅱ)—α-hydroxide with a turbostratic structure [J]. Journal of Power Sources, 1991, 35: 263-277.

[16] Faure C, Borthomieu Y, Delmas C. Infrared characterization of turbostratic α- and well crystallized α^*-cobalted nickel hydroxides [J]. Journal of Power Sources, 1991, 36: 113-125.

[17] Faure C, Delmas C, Fouassier M. Characterization of a turbostratic α-nickel hydroxide quantitatively obtained from an NiSO$_4$ solution [J]. Journal of Power Sources, 1991, 35: 279-290.

[18] Lu P W T, Srinivasan S. Electrochemical-ellipsometric studies of oxide film formed on nickel during oxygen evolution [J]. Journal of the Electrochemical Society, 1978, 125: 1416-1422.

[19] Miao H J, Piron D L. Electro-deposition of catalytically active nickel for the oxygen evolution reaction-effects of anionic composition [J]. Journal of the Electrochemical Society, 1992, 139 (10): 2697-2704.

(Edited by LI Xiang-qun)